Energy 94 (2016) 666–671

Contents lists available at ScienceDirect

Energy

journal homepage: www.elsevier.com/locate/energy

Pyrolytic cyanobacteria derived activated carbon as high performance electrode in symmetric supercapacitor

Keliang Wang [a], Yuhe Cao [a], Xiaomin Wang [a], Qihua Fan [b, **], William Gibbons [c], Tylor Johnson [c], Bing Luo [d], Zhengrong Gu [a, *]

[a] Agricultural and Biosystems Engineering Department, South Dakota State University, Brookings, SD 57007, United States
[b] Electrical Engineering and Computer Science Department, South Dakota State University, SD 57007, United States
[c] Biology and Microbiology Department, South Dakota State University, Brookings, SD 57007, United States
[d] Characterization Facility of the University of Minnesota, Minneapolis, MN 55455, United States

ARTICLE INFO

Article history:
Received 2 July 2015
Received in revised form
28 September 2015
Accepted 14 October 2015
Available online 17 December 2015

Keywords:
Cyanobacteria
Pyrolysis
Supercapacitor

ABSTRACT

Cyanobacteria, as a renewable source of carbon, was used to prepare activated carbon electrodes in supercapacitors. The activation includes a pre-carbonization at 400 °C followed by KOH heat treatment at 800 °C, leading to efficient and high degree of graphitization. The activated carbon electrode consisted primarily of carbon and oxygen, and possessed a large specific surface area of 2184 $m^2 g^{-1}$, with pore size centered at 27 nm. In 6 mol L^{-1} KOH electrolyte, the electrode exhibited superior specific capacitance of 271 F g^{-1} and 222 F g^{-1} at a charge/discharge current density of 0.1 A g^{-1} and 5.0 A g^{-1}, respectively. The results demonstrated that the activated carbon derived from cyanobacteria can serve as promising electrode material for electrical double-layer capacitors.

1. Introduction

Carbon materials are widely used as electrode materials in EDLC (electric double layer capacitors) [1], due to their high electric conductivity and excellent tolerance to various electrolytes. EDLC, stores energy by reversible adsorption of ions at the interface between electrolyte and active electrode materials. Currently, carbon black, single and multiwall carbon tubes and graphene are the predominant materials used in EDLC [2,3]. However, these materials have several drawbacks, such as low SSA (specific surface area) and high cost, which limit their potential applications. The capacitance of EDLC is closely related to three factors: i) accessible SSA of the electrode; ii) type of the electrolyte; and iii) effective thickness of the double layer. These factors are illustrated in the formula below [4]:

$$C = \frac{\varepsilon_r \varepsilon_0 A}{d} \quad (1)$$

where C (F) is the capacitance of the EDLC, ε_r (F m^{-1}) is the dielectric constant of electrolyte, ε_0 (F m^{-1}) is the dielectric constant of vacuum, d (m) is the effective thickness of the double layer, and A (m^2) is the electrode surface area. It should be noted that only the surfaces that are accessible to the electrolyte ions can contribute to charge storage. Therefore, optimization of the pore size, pore structure, surface properties and conductivity of the electrode materials is required [4].

Carbon materials derived from biomass are promising candidates for EDLC electrodes due to their materials' abundance, low cost, sustainability and possible large SSA. Activated carbon produced from biomass can be divided into two groups: physically activated and chemically activated. Physically activated carbon is obtained by treating biomass with steam or CO_2 under a prescribed temperature, while chemically activated carbon is prepared by exposing biomass to activating agent (*e. g.* KOH, H_3PO_4, $ZnCl_2$) at high temperatures [5–8]. Physical activation typically results in activated carbon with larger SSA. Chemical activation typically results in activated carbon with greater amount of surface functional groups. Both of these characteristics would enhance EDLC performance. Therefore, various naturally abundant biomass and biowaste have been studied for supercapacitor electrodes [9,10].

Cyanobacteria are phototrophic bacteria that exist in many ecosystems across the planet. They have existed on Earth for

* Corresponding author. Tel./fax: +1 605 688 5372.
** Corresponding author. Tel./fax: +1 605 688 5910.
E-mail addresses: qihua.fan@sdstate.edu (Q. Fan), zhengrong.gu@sdstate.edu (Z. Gu).

http://dx.doi.org/10.1016/j.energy.2015.10.047
0360-5442/

approximately 3.5 billion years, and are a key contributor to global photosynthesis. However, not all cyanobacterias are beneficial to environment and human health; some cyanobacteria grow and expand too fast, destroying fresh water and creating toxins [11]. In recent years, the rapid and efficient photosynthetic system of cyanobacteria has been re-directed by metabolic engineering to produce third-generation biofuels and long-chain hydrocarbon intermediates [12,13]. Furthermore, cyanobacteria has been recognized as the most promising source of biomass for producing next generation biofuel because it can be easily grown in recirculating photobioreactors fed with CO_2 and powered by sunlight [14,15] without competing for crop land and fresh water [16]. In most current and proposed cyanobacteria bioenergy or biofuel platforms, cyanobacteria biomass is left as waste after harvesting lipid based biodiesel or volatile biofuels. Therefore, utilization of cyanobacteria biomass as feedstock for advanced materials or other high value products must be developed. Due to the abundance and accessibility of cyanobacteria, it is attractive to verify the suitability of converting this biomass into active carbon for energy storage. To our knowledge, no research has been attempted to use cyanobacteria for supercapacitors electrodes but seaweeds and microalgae [17,18]. The goal of this work was to evaluate cyanobacteria as a renewable source of carbon to create EDLC electrodes and transform the waste into efficient energy storage materials. In this work, we first activated cyanobacteria biomass *via* KOH chemical treatment, and then used the activated carbon to prepare EDLC electrode. We systematically evaluated the materials structures and properties (*e. g.* SSA, pore size, electric conductivity, and surface functional groups) that accounted for the promising EDLC performance.

2. Experimental

2.1. Preparation of activation and original carbon

All reagents were purchased from Fisher Scientific Incorporation. Cyanobacteria cell mass was obtained from Biology and Microbiology department of South Dakota State University. To prepare the activated carbon, 10 g dried cyanobacteria powder was heated to 400 °*C* for 1 h in a muffle furnace (1100 box furnace, Lindberg/Blue M, Thermo Scientific Inc.) using N_2 as inert carrier gas (flow rate was 96 ml min^{-1}) to complete the pre-carbonization. After the carbonized material was cooled to room temperature, it was mixed with activation agent KOH in a mass ratio of 1:3 in a steel crucible. To obtain a uniform mixture, 30 mL deionized water was also added. The mixture was left in the crucible and dried in an oven with stirring every 20 min at 110 °*C* for 24 h. Then, the crucible was transferred into a muffle and annealed at 800 °*C* for 1 h under a N_2 flow rate of 96 mL min^{-1}. Afterwards, the activated carbon was washed with deionized water to remove the extra KOH for several times till pH equals 7. After this, the sample was hydrothermally treated with 0.1 mol L^{-1} HCl at 110 °*C* for 1 h in a 50 mL PTFE (polytetrafluoroethylene) autoclave to remove the residual KOH and other impurities. Finally, the material was washed several times with deionized water again till to pH stabilized at 7. The obtained material was dried at 105 °*C* for 12 h in an oven and denoted as AC (activated carbon). For comparison, the OC (original carbon) materials were also prepared in the same way, except the KOH treatment was omitted.

2.2. Preparation of electrodes

Electrodes were prepared by mixing 80 *wt%* AC or OC with 10 *wt* % acetylene black (that to improve the conductivity), and 10 *wt%* PTFE served as binder, and then pressing onto nickel foam current collector (EQ-bcnf-16m, MTI Corp.) of a surface area of 1 cm^2. The electrodes were dried at 60 °*C* overnight in an oven. Afterwards, a sandwich structure was formed placing two pieces of microporous PP (Polypropylene) separator celgard-3501 between two electrodes in a cell 2032 coin-type system. Finally, the cell was pressed under a pressure of 1000 kg cm^{-2} to finish the assembly.

2.3. Physical characterization

XPS (X-ray photoelectron spectra) was obtained using a SSX-100 system (Surface Science Laboratories, Inc.) equipped with a monochromated AlK_α X-ray source, a HSA (hemispherical sector analyzer) and a resistive anode detector. For high resolution data, the lowest binding-energy C 1s peak was set at 285.0 eV and used as the reference for all of the other elements. Raman spectrum was obtained on a Horiba LABRam confocal Raman microscopean with excitation wavelength at 532 nm from a diode pumped solidstate laser. Isothermal adsorption analyses with N_2 were carried out at 77 K (liquid nitrogen bath), using Tristar 3000 Micropore analyzer. The specific surface area was determined by the BET (Brunauer–Emmett–Teller) method and the pore size distribution was calculated by the DFT (density functional theory) method using NLDFT (non local density functional theory) analysis for carbon with slit pore model (Micromeritics Inc.) TEM (Transmission Electron Microscope) (Talos F200X, FEI Inc.) equipped with EDX (energy-dispersive X-ray spectroscopy) was used to study the morphology, microstructure, and elemental mapping of the materials at an acceleration voltage of 80 kV.

2.4. Electrochemical characterization

CV (Cyclic voltammetry) and electrochemical impedance spectroscopy measurements were performed on an electrochemical work station (SP-150, BioLogical, France) in 6 mol L^{-1} KOH electrolyte. The galvanostatic charge/discharge curves were obtained from BTS series battery test system (NEWARE, China).

To evaluate the specific capacitance in the two-electrode system, the following equation [19] was used:

$$C = \frac{2I\Delta t}{m\Delta v} \tag{2}$$

where C (F g^{-1}) is the specific capacitance, I (A) is the charge/discharge current, Δt (s) is the corresponding charge or discharge time, m (g) is the mass of active materials on single electrode, and Δv(V) is the total corresponding potential change.

3. Results and discussion

Fig. 1a shows the N_2 sorption–desorption isotherms of AC and pore size distribution in the inset. The AC exhibited an extremely large BET SSA (up to 2184 m^2 g^{-1}) and desirable pore structure. The large SSA means there is a large accessible surface area for the electrolyte, while the narrow pore size distribution (which concentrates at 27 nm) can serve as ion-buffering reservoir and allow the smooth transform of ions [20]. Fig. 1b presents the Raman spectra of AC. Two featured peaks correspond to *D* band (1340 cm^{-1}) and *G* band (1585 cm^{-1}) and these were relate to i) the breaking of the A_{1g} symmetry caused by structural disorder and defects and ii) the in-plane bond −stretching motion of a pair of sp^2 carbon atoms with E_{2g} symmetry, respectively [21].

XPS survey was employed to confirm the contained elements and corresponding existing forms. As shown in Fig. 1c, the signals of C and O were detected. The high-resolution XPS spectra of the C 1s region is illustrated in Fig. 1d. The different binding energies

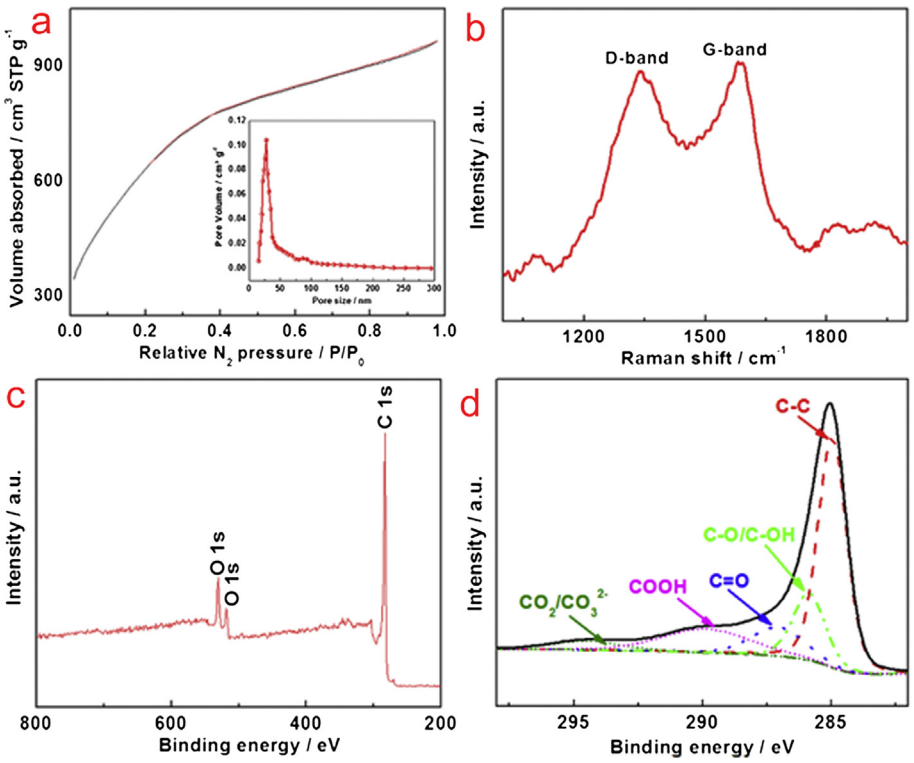

Fig. 1. N_2 sorption–desorption isotherms (a), Raman spectra (b), XPS survey spectra (c) and C 1s XPS spectra of AC (d). The inset in (a) is the pore size distribution plot.

indicated that the C atoms were linked to one O atom by a single bond, a double bond, or two oxygen atoms [22]. Deconvolution of the C 1s spectra showed the most pronounced peak being graphite-like carbon (C–C). The peaks located at different binding energies were attributed to different oxygen-containing groups *e.g.*, C–O/C–OH (~286 eV), C=O (~287 eV), COOH (~289 eV), and CO_2/CO_3^{2-} (~294 eV) [23]. These surface functional groups can improve the hydrophilic nature of the AC, thus allowing easy access of the electrolyte to the narrow pores size, which concentrated at 27 nm.

The morphology and content of the AC and OC samples were investigated by TEM. Fig. 2a and b showed that the OC structure had disordered structures that appear overlapped. In contrast, the AC exhibited a narrower pore size distribution, and consisted mostly of graphite (Fig. 2c) and pores (Fig. 2d). The fringes of the graphite crystallite were also distinctly presented in Fig. 2d, indicating a high degree of graphitization. The significant difference between OC and AC can be assigned to the contribution of KOH, as K and K compounds become intercalated into the carbon lattices of the carbon matrix during activation, resulting in the expansion of the carbon lattices [24]. EDX elemental mapping (Fig. 2e, f and g) depict the spatial distribution of the constituting elements within AC. Both C and O are distributed in the sample, and the ingredients are consistent with the result of XPS survey.

To evaluate the electrochemical performance of the prepared electrodes in assembled supercapacitor. CV, galvanostatic charge/discharge, EIS (electrochemical impedance spectroscopy) and cycle life tests were conducted in a 6 mol L^{-1} KOH electrolyte. The CV curves of OC and AC at various scanning rates ranging from 10 to 300 mV s^{-1} were shown in Fig. 3 a and c, respectively. In contrast to OC, AC displayed more rectangular shape, which is an indication of a typical EDLC behaviour. A high specific capacitance of 271 F g^{-1} (calculated based on formula 1) was reached at low scan rate of 10 mV s^{-1}, and a capacitance remained as large as 222 F g^{-1} even at a high scan rate of 300 mV s^{-1} for AC electrode. The specific capacitance was much higher than OC at either low or high scanning rate. Therefore, the activation was effective and cause changes (such as specific surface area, porous structure, and degree of graphitization) that greatly facilitated an improvement in the specific capacitance improvement. In addition, compared to the performance of N-doped carbon materials derived from biomass, the AC still exhibited outstanding performance even without N doping (as shown in Table 1).

Fig. 3b and d showed the galvanostatic charge/discharge plots at different current densities of 0.1, 0.5, 1.0, and 5.0 A g^{-1} for OC and AC electrodes, respectively. For both materials, the charging and discharging curves were symmetric at the tested current densities, demonstrating that they possesses excellent capacitive reversibility as EDLC electrode. It is noteworthy that there was apparently a large *IR* drop (internal resistance drop) from 0.9 to 0.8 V for both OC and AC electrodes at 0.1 A/g. However, as compared to OC, AC produced more symmetrical triangle shaped galvanostatic charge–discharge curves with a lower *IR* drop, indicating lower internal resistance and less heat produced from wasted energy during charge/discharge [31].

The EIS (electrochemical impedance spectroscopy) (Fig. 3e) was measured in a frequency range from 100 mHz to 100 kHz to further characterized the resistance for OC and AC. The resistance consisted of bulk electrolyte resistance (0.27 and 0.35 Ω), interfacial resistance (0.57 and 0.3 Ω), and apparent resistance of intra-particle pores (4.1 and 0.7 Ω) [32] for OC and AC electrodes, respectively. These values were determined from the *x*-axis value from the intercept, semicircle and 45°region, respectively. As the resistance rooted from electrolyte, interfaces and pores and was of great importance in energy storage devices, smaller resistance implied better electrical conductivity of the carbon matrix and suitable pore structure for ion transference.

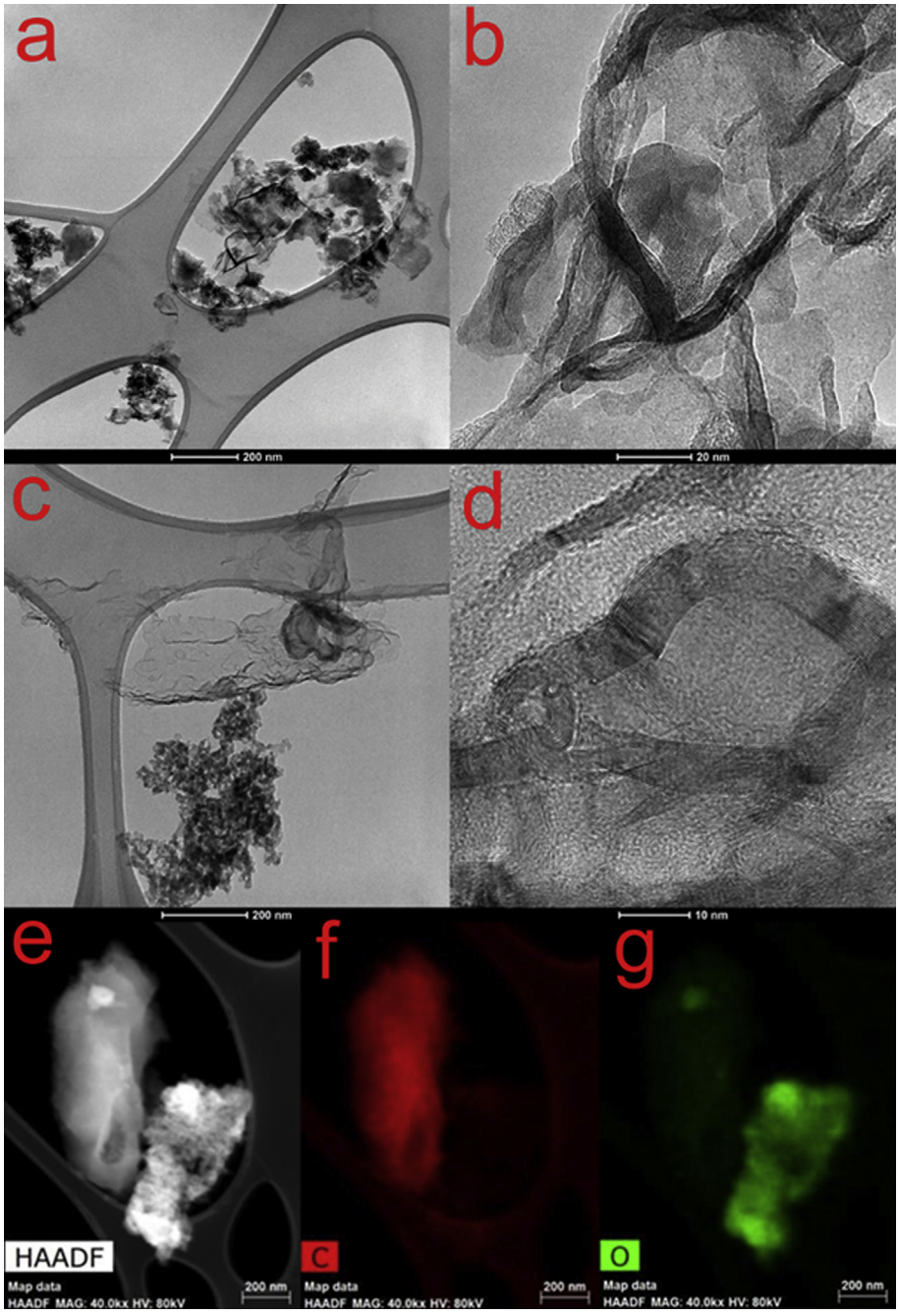

Fig. 2. TEM images of different magnifications for OC (a, b) and AC (c, d), and HAADF-STEM (High Angle Annulau Dark Field-Svanning Transmission Electron Microscope) image of spatially resolved EDX elemental maps (e–g) depicting the spatial distribution of the constituting elements within AC: carbon and oxygen maps. Note: The unit "a.u." in (b), (c), and (d) means arbitrary unit, which is the relative signal intensity detected.

Then stability of supercapacitors was yet another significant index to access their performance. The OC and AC electrode at different current densities ranging from 0.1 to 5 A g^{-1} was assessed by the cycle life test (Fig. 3f). The specific capacitance in 1000 cycles was recorded for each charge/discharge current density. After 1000 cycles, both OC and AC showed almost 100% retention of specific capacitance at individual charge/discharge current density, indicating superior stability of AC as EDLC electrodes. However, the specific capacitance of AC was far higher than that of OC. The electrochemical measurements confirmed that cyanobacteria based AC is a promising EDLC electrode material.

4. Conclusion

We have successfully derived activated carbon from cyanobacteria (a bio waste material) *via* chemical activation and demonstrated that the activation carbon can be used as high performance electrodes in supercapacitors. The electrodes resulted in a high specific capacitance of 271 F g^{-1} at a charge/discharge current density of 0.1 A g^{-1}, which is even better than the nitrogen doped carbon electrode. The specific capacitance retention ratio was maintained at almost 100% at each individual charge/discharge current density ranging from 0.1 to 5 A g^{-1}, implying good stability. Considering its extraordinary

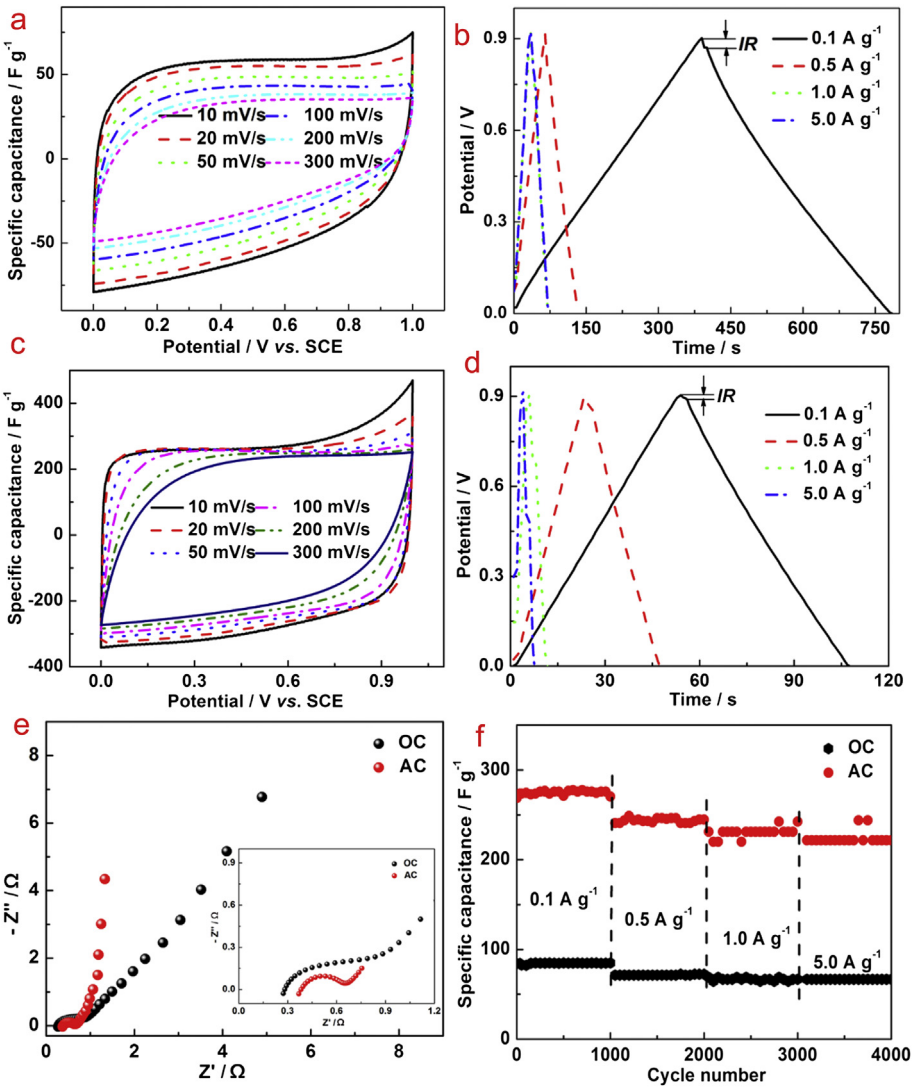

Fig. 3. CV curves (a, c) at various scanning rates ranging from 10 to 300 mV s^{-1}, galvanostatic charge/discharge curves (b, d) at different current density ranging from 0.1 to 5 A g^{-1}, Nyquist plot (e), and cycle life plot (f) at different current density ranging from 0.1 to 5 A g^{-1} for OC and AC electrodes in 6 mol L^{-1} KOH electrolyte, respectively.

Table 1
Comparison of specific capacitance of different carbon materials.

Electrode materials	Electrode system	Specific capacitance	Current density	Electrolyte	Reference
N-doped graphene hollow nanospheres	3	381 F g^{-1}	1 A g^{-1}	6 M KOH	[25]
N-Doped ordered mesoporous carbon	3	227 F g^{-1}	0.2 A g^{-1}	6 M KOH	[26]
Porous N-doped hollow carbon spheres	3	213 F g^{-1}	0.5 A g^{-1}	6 M KOH	[27]
N-doped porous carbon	2	245 F g^{-1}	0.05 A g^{-1}	6 M KOH	[28]
N-modified few-layer graphene	3	227 F g^{-1}	1 A g^{-1}	6 M NaOH	[29]
Hierarchical N-doped porous carbon	3	198 F g^{-1}	1 A g^{-1}	6 M KOH	[7]
N-doped porous carbon nanofibers	3	202 F g^{-1}	1 A g^{-1}	6 M KOH	[30]
AC	2	271/222 F g^{-1}	0.1/1 A g^{-1}	6 M KOH	This work

electrochemical performance in supercapacitors, transformation of bio-waste to energy storage material in this work can inspire more applications into other fields like non-precious electrocatalyst of fuel cell.

Acknowledgement

This research was funded by USDA-NIFA Agriculture and Food Research Initiative Sustainable Bioenergy Program (2011-67009-20030) NSF EpsCor Track II Dakota BioCon center and was also partly supported by NSF award #1462389.

References

[1] Li Q, Jiang R, Dou Y, Wu Z, Huang T, Feng D, et al. Synthesis of mesoporous carbon spheres with a hierarchical pore structure for the electrochemical double-layer capacitor. Carbon 2011;49:1248–57.
[2] Basirico L, Lanzara G. Moving towards high-power, high-frequency and low-resistance CNT supercapacitors by tuning the CNT length, axial deformation and contact resistance. Nanotechnology 2012;23:305401.

[3] Kossyrev P. Carbon black supercapacitors employing thin electrodes. J Power Sources 2012;201:347–52.
[4] Zhai Y, Dou Y, Zhao D, Fulvio PF, Mayes RT, Dai S. Carbon materials for chemical capacitive energy storage. Adv Mater 2011;23:4828–50.
[5] Chen M, Kang X, Wumaier T, Dou J, Gao B, Han Y, et al. Preparation of activated carbon from cotton stalk and its application in supercapacitor. J Solid State Electr 2013;17:1005–12.
[6] He X, Li R, Han J, Yu M, Wu M. Facile preparation of mesoporous carbons for supercapacitors by one-step microwave-assisted $ZnCl_2$ activation. Mater Lett 2013;94:158–60.
[7] Hong X, Hui K, Zeng Z, Hui K, Zhang L, Mo M, et al. Hierarchical nitrogen-doped porous carbon with high surface area derived from endothelium corneum gigeriae galli for high-performance supercapacitor. Electrochim Acta 2014;130:464–9.
[8] Mladenov M, Alexandrova K, Petrov NV, Tsyntsarski B, Kovacheva D, Saliyski N, et al. Synthesis and electrochemical properties of activated carbons and $Li_4Ti_5O_{12}$ as electrode materials for supercapacitors. J Solid State Electr 2013;17:2101–8.
[9] Peng C, Yan X-b, Wang R-t, Lang J-w, Ou Y-j, Xue Q-j. Promising activated carbons derived from waste tea-leaves and their application in high performance supercapacitors electrodes. Electrochim. Acta 2013;87:401–8.
[10] Rufford TE, Hulicova-Jurcakova D, Zhu Z, Lu GQ. Nanoporous carbon electrode from waste coffee beans for high performance supercapacitors. Electrochem Commun 2008;10(10):1594–7.
[11] Barrington DJ, Ghadouani A. Application of hydrogen peroxide for the removal of toxic cyanobacteria and other phytoplankton from wastewater. Environ Sci Technol 2008;42(23):8916–21.
[12] Li Y, Horsman M, Wu N, Lan CQ, Dubois-Calero N. Biofuels from microalgae. Biotechnol Prog 2008;24:815–20.
[13] Robertson DE, Jacobson SA, Morgan F, Berry D, Church GM, Afeyan NB. A new dawn for industrial photosynthesis. Photosynth Res 2011;107:269–77.
[14] González LC, Acién FF, Fernández SJ, Sánchez FJ, Cerón GM, Molina GE. Utilization of the cyanobacteria Anabaena sp. ATCC 33047 in CO_2 removal processes. Bioresour Technol 2009;100:5904–10.
[15] Qiang H, Richmond A. Productivity and photosynthetic efficiency of spirulina platensis as affected by light intensity, algal density and rate of mixing in a flat plate photobioreactor. J Appl Phycol 1996;8:139–45.
[16] Sarsekeyeva F, Zayadan BK, Usserbaeva A, Bedbenov VS, Sinetova MA, Los DA. Cyanofuels: biofuels from cyanobacteria. Reality and perspectives. Photosynth Res 2015:1–12.
[17] Raymundo-Piñero E, Cadek M, Beguin F. Tuning carbon materials for supercapacitors by direct pyrolysis of seaweeds. Adv Funct. Mater 2009;19(7):1032–9.
[18] Sevilla M, Gu W, Falco C, Titirici M, Fuertes A, Yushin G. Hydrothermal synthesis of microalgae-derived microporous carbons for electrochemical capacitors. J Power Sources 2014;267:26–32.
[19] Wahid M, Parte G, Phase D, Ogale S. Yogurt: a novel precursor for heavily nitrogen doped supercapacitor carbon. J Mater Chem A 2015;3(3):1208–15.
[20] Ning X, Zhong W, Li S, Wang Y, Yang W. High performance nitrogen-doped porous graphene/carbon frameworks for supercapacitors. J Mater Chem A 2014;2(23):8859–67.
[21] Qi J, Jiang L, Wang S, Sun G. Synthesis of graphitic mesoporous carbons with high surface areas and their applications in direct methanol fuel cells. Appl Catal B Environ 2011;107:95–103.
[22] Moreno-Castilla C, Lopez-Ramon M, Carrasco-Marın F. Changes in surface chemistry of activated carbons by wet oxidation. Carbon 2000;38:1995–2001.
[23] Ding JD, Diao YF, Shen HG. Characters of nickel-loaded activated carbon fibers and adsorption experiments of gaseous mercury. Adv Mater Res 2011;156:1211–4.
[24] Romanos J, Beckner M, Rash T, Firlej L, Kuchta B, Yu P, et al. Nanospace engineering of KOH activated carbon. Nanotechnology 2012;23. 015401.
[25] Fan W, Xia Y-Y, Tjiu WW, Pallathadka PK, He C, Liu T. Nitrogen-doped graphene hollow nanospheres as novel electrode materials for supercapacitor applications. J Power Sources 2013;243:973–81.
[26] Wei J, Zhou D, Sun Z, Deng Y, Xia Y, Zhao D. A controllable synthesis of rich nitrogen-doped ordered mesoporous carbon for CO_2 capture and supercapacitors. Adv Funct. Mater 2013;23:2322–8.
[27] Han J, Xu G, Ding B, Pan J, Dou H, MacFarlane DR. Porous nitrogen-doped hollow carbon spheres derived from polyaniline for high performance supercapacitors. J Mater Chem A 2014;2:5352–7.
[28] Xu B, Zheng D, Jia M, Cao G, Yang Y. Nitrogen-doped porous carbon simply prepared by pyrolyzing a nitrogen-containing organic salt for supercapacitors. Electrochim Acta 2013;98:176–82.
[29] Xiao N, Lau D, Shi W, Zhu J, Dong X, Hng HH, et al. A simple process to prepare nitrogen-modified few-layer graphene for a supercapacitor electrode. Carbon 2013;57:184–90.
[30] Chen L-F, Zhang X-D, Liang H-W, Kong M, Guan Q-F, Chen P, et al. Synthesis of nitrogen-doped porous carbon nanofibers as an efficient electrode material for supercapacitors. ACS Nano 2012;6:7092–102.
[31] Wu Q, Xu Y, Yao Z, Liu A, Shi G. Supercapacitors based on flexible graphene/polyaniline nanofiber composite films. ACS Nano 2010;4:1963–70.
[32] Yoo HD, Jang JH, Ryu JH, Park Y, Oh SM. Impedance analysis of porous carbon electrodes to predict rate capability of electric double-layer capacitors. J Power Sources 2014;267:411–20.